Applied Radiation and Isotopes 174 (2021) 109778

Contents lists available at ScienceDirect

Applied Radiation and Isotopes

journal homepage: www.elsevier.com/locate/apradiso

In vivo preclinical assessment of novel ^{68}Ga-labelled peptides for imaging of tumor associated angiogenesis using positron emission tomography imaging

Noémi Dénes [a,b], Adrienn Kis [a,c], Judit P. Szabó [a,c], István Jószai [a], István Hajdu [a], Viktória Arató [a], Kata Nóra Enyedi [d], Gábor Mező [d,e], János Hunyadi [f], György Trencsényi [a,b,c,1], István Kertész [a,*,1]

[a] Division of Nuclear Medicine and Translational Imaging, Department of Medical Imaging, Faculty of Medicine, University of Debrecen, Nagyerdei St. 98, H-4032, Debrecen, Hungary
[b] Gyula Petrányi Doctoral School of Allergy and Clinical Immunology, Faculty of Medicine, University of Debrecen, Nagyerdei St. 98, H-4032, Debrecen, Hungary
[c] Doctoral School of Clinical Medicine, Faculty of Medicine, University of Debrecen, Nagyerdei St. 98, H-4032, Debrecen, Hungary
[d] Eötvös Loránd University, Faculty of Science, Institute of Chemistry, Budapest, Hungary
[e] MTA-ELTE, Research Group of Peptide Chemistry, Hungarian Academy of Sciences, Eötvös L. University, Budapest, Hungary
[f] Department of Dermatology, Faculty of Medicine, University of Debrecen, Nagyerdei St. 98, H-4032, Debrecen, Hungary

ARTICLE INFO

Keywords:
Aminopeptidase N/CD13
VEGFR-1
Angiogenesis
Peptides
^{68}Ga
Radiolabelling
PET imaging

ABSTRACT

Formation and growth of metastases require a new vascular network. Angiogenesis plays an essential role in the expansion and progression of most malignancies. A high number of molecular pathways regulate angiogenesis, including vascular endothelial growth factor (VEGF), $\alpha_v\beta_3$ integrin, matrix metalloproteinases (MMPs), or aminopeptidase N. The aim of this study is to involve new, easily accessible peptide sequences into the of neo-angiogenesis in malignant processes. Labelling of these peptide ligands with ^{68}Ga enable PET imaging of neo-vascularization.

1. Introduction

Angiogenesis is fundamental in the progression of cancer, and promote the formation of metastatic lesions (Simons, 2005; Folkman, 1971; Nishida et al., 2006). This complicate mechanism is regulated by a balance between pro- and anti-angiogenic factors (Ellis et al., 2002; Kazerounian et al., 2018). Therefore, non-invasive detection of this process has a great importance in the early diagnosis of different malignancies. Hence, promising biologic targets for the specific imaging of angiogenesis can involve different endothelial cell markers of angiogenesis, non-endothelial cells contributing to neovascularization, and markers of the extracellular matrix (Denekamp, 1993; Ellis et al., 2001). Previous studies demonstrated the presence of the aminopeptidase N (CD13) – a zinc-dependent membrane-bound ectopeptidase - on the new tumor vasculatures (Pasqualini et al., 2000; Luan and Xu, 2007). High expression of CD13 can be found in several human solid tumors, including melanoma (van Hensbergen et al., 2004), prostate-, lung- and ovarian cancer (Chen et al., 2013). A strong correlation was determined between the CD13 expression and the invasive feature of the tumors. Novel specific markers of angiogenic endothelium, and CD13 have been identified by phage display experiments in tumor models. The peptide motif, NGR (Asn-Gly-Arg) has been shown to home specifically to tumor vessels in xenografted animal models but not other CD13-rich tissues (Arap et al., 1998; Wang et al., 2011; von Wallbrunn et al., 2008), despite CD13 is expressed in various normal tissues also. The reason of this particular behaviour can be due to the expression of different forms of CD13. It has formerly been demonstrated that the cyclic form of NGR has approximately ten-fold higher targeting efficacy than linear versions of the identical peptide sequence for targeting various tumors (Colombo et al., 2002). These results suggest that NGR-containing peptides labelled with positron emitting nuclides can be a useful predictive

* Corresponding author. Division of Nuclear Medicine and Translational Imaging, Department of Medical Imaging, Faculty of Medicine, University of Debrecen, 4032, Debrecen, Nagyerdei krt. 98. Debrecen, Hungary.
E-mail address: kertesz.istvan@med.unideb.hu (I. Kertész).
[1] these authors contributed equally to the study.

https://doi.org/10.1016/j.apradiso.2021.109778
Received 23 December 2020; Received in revised form 27 April 2021; Accepted 7 May 2021
Available online 12 May 2021

Abbreviations

ACN acetonitrile
ANOVA analysis of variance
APN/CD13 aminopeptidase N (CD13)
APRPG alanyl-prolinyl-argininyl-prolinyl-glycyl
ATCC american type culture collection
c(KNGRE)-NH2 cyclic(lysyl-asparaginyl-glycyl-argininyl-glutamic acid amide)
ClTrt chlorotrityl
DIC/HOBt diisopropylcarbodiimide/ 1-hydroxybenzotriazole
DIPEA N,N-Diisopropylethylamine
DMEM dulbecco's modified eagle medium
DMF N,N-Dimethylformamide
DOTA 1,4,7,10-Tetraazacyclododecane-1,4,7,10-tetraacetic acid
ESI-MS electrospray ionisation mass spectrometry
FBS fetal bovine serum
Fmoc-Arg(Pbf)-OH Nα-Fmoc-Nω-(2,2,4,6,7-pentamethyldihydrobenzofuran-5-sulfonyl)-L-arginine, Nα-Fmoc-Nω-Pbf-L-arginine
He/De rat hepatocellular carcinoma
HLB hydrophilic-lipophilic-balanced
Maleimide-NODAGA Maleimide-1,4,7-triazacyclononane,1-glutaric acid-4,7-acetic acid
MEM non-essential amino acid
Ne/De rat mesoblastic nephroma
NGR asparaginyl-glycyl-arginine
NODAGA 1,4,7-triazacyclononane,1-glutaric acid-4,7-acetic acid
NODAGA-c(NGR) c[Lys(NODAGA)-Asn-Gly-Arg-Glu]-NH2
NOTA 1,4,7-triazacyclononane-triacetic acid
NOTA-c(NGR) c[Lys(NOTA)-Asn-Gly-Arg-Glu]-NH2
PET positron emission tomography
p-SCN-Bn-NODAGA S-2-(4-isothiocyanatobenzyl)-1,4,7-triazacyclononane-1-glutaric acid-4,7-acetic acid
p-SCN-Bn-NOTA 2-S-(4-Isothiocyanatobenzyl)-1,4,7-triazacyclononane-1,4,7-triacetic acid
RP-HPLC reversed phase-high pressure liquid chromatography
SPPS solid phase peptide synthesis
SUVmean standardized uptake value (mean)
T/M tumor-to-muscle ratio
TFA trifluoroacetic acid
TIS triisopropylsilane
YEVGHRC tyrosinyl-glutamic acidyl-valinyl-glycyl-histidinyl-argininyl-cystene

diagnostic agent or, applying therapeutic isotopes they can serve as promising tools against the tumors. On the other hand, it is well known that the NGR sequence, has a strong propensity to undergo deamidation of Asn side chain (Meinwald et al., 1986), and the process can lead to the formation of isoAsp and Asp residues (Kirikoshi et al., 2017). Despite of the stability issue of the NGR motif, in the literature one can see several NGR analogues labelled with different radionuclides through different bifunctional chelators. The most studied nuclides were ^{68}Ga (Zhang et al., 2014; Máté et al., 2015; Shao et al., 2014; Zhao, 2016) and ^{64}Cu (Chen et al., 2013; Li et al., 2014) for positron emission tomography (PET) imaging but one can find examples for the application of ^{99m}Tc (Ma et al., 2013) for single-photon emission computed tomography (SPECT) imaging.

The vascular endothelial growth factor receptor- (VEGFR-1) is also one of the key molecules in the process of tumor-associated neo-angiogenesis. The VEGFR-1 – as a tyrosine kinase transmembrane receptor – is overexpressed in several human cancers, furthermore, due to VEGFR-1 plays an important role in tumor neo-angiogenesis, in the inhibition of apoptosis and, in the induction of chemoresistance, the presence of this receptor in the tumors predicts poor prognosis in patients (Graziani et al., 2016).

Therefore, the discovery of easily available and less susceptible peptide sequences targeting the neo-angiogenetic processes can have a great impact. In this work we aimed to involve into our research area new linear sequences, which can serve as a lead compound for further radioligand development. In this proof-of-concept type study the APN selective peptide LN peptide (YEVGHRC) (Jia et al., 2017) and the VEGFR-1 selective APRPG (Oku et al., 2002) were conjugated with macrocyclic chelators and were labelled with ^{68}Ga.

The PET-isotope, ^{68}Ga bears close to ideal physical properties, furthermore it is easily accessible via ^{68}Ge/^{68}Ga-generators and offers well-established complexation chemistry for the labelling of biomolecules (Velikyan, 2013; Smith et al., 2013; Banerjee and Pomper, 2013). The Ga^{3+} ion can be complexed by macrocyclic and acyclic chelators also and its most common coordination number is six. DOTA is one of the most widely used chelators which is applied for complexing radioactive metals. However, due to the size of the ring, and the existing 8 donor atoms it is better suited for complexation with larger cations (Bi^{3+}, Y^{3+}, Sc^{3+}). The labelling with ^{68}Ga at room temperature is extremely slow and it is incompatible with the half-life of ^{68}Ga.

The NOTA-type chelator family is excellent for complexing Ga^{3+} due to the appropriate ring size and coordination number. The NOTA chelator provides quantitative radiolabelling with ^{68}Ga at room temperature. NODAGA carries an extra carboxyl group than NOTA and has even more hydrophilic character than the former, which can influence beneficially the biological behaviour of radiotracer (Satpati et al., 2018). Therefore, during our research, we selected NODAGA from the NOTA family, as a chelator to conjugate various, neo-angiogenesis-selective peptide derivatives and then radiolabel the substances with ^{68}Ga. Moreover, we have evaluated the isotope-labelled peptide-derivatives *in vivo*, as an imaging biomarker of angiogenesis in different tumor models and using them in preclinical imaging studies.

2. Materials and methods

2.1. Materials

The chemicals for the peptide-synthesis and for the HPLC-purification were ordered from Reanal (Budapest, Hungary), IRIS Biotech GmbH (Marktredwitz, Germany) and Molar Chemicals Kft (Halásztelek, Hungary). The ^{68}Ge/^{68}Ga generator was produced by Eckert-Ziegler, GalliaPharm® (Berlin, Germany). The *p*-SCN-Bn-NOTA, *p*-SCN-Bn-NODAGA and Maleimide-NODAGA macrocyclic chelators were obtained for CheMatech (Dijon France), the HCl, NaOAc buffer and water were Ultrapure quality and were purchased from Merck KGaA (Darmstadt, Germany). Oasis HLB 1 cc cartridge was the product of Waters Corporation (Massachusetts, USA). All other reagents and solvents were the products of Sigma-Aldrich Kft. (Budapest, Hungary) and were analytical grade, moreover we used them without further purification every case.

2.2. Synthesis of peptide APRPG-NH_2 and APRPG-COOH

The APRPG-NH_2 peptide was prepared on Rink-Amide MBHA resin while the APRPG-COOH peptide was synthesized on 2-ClTrt resin by SPPS, using standard Fmoc-chemistry. The only side chain protected amino acid derivative was Fmoc-Arg(Pbf)-OH. The mixture of 2% DBU and 2% piperidine in DMF was applied for the removal of Fmoc protecting group and for the coupling of amino acid derivatives DIC/HOBt coupling agents (3 equivalent each) were used. The free peptides were

cleaved from the resins with 95% TFA, 2.5% water and 2.5% TIS as cleavage cocktail. The crude peptides were purified by RP-HPLC and the pure compounds were analysed by analytical RP-HPLC and ESI-MS. The yield of the end products was over 70% in both cases.

2.3. Mass spectrometry

Electrospray (ESI)-mass spectrometric analyses were carried out on an Esquire 3000+ ion trap mass spectrometer (Bruker Daltonics, Bremen, Germany). Spectra were acquired in the 50–2500 *m/z* range. Samples were dissolved in a mixture of ACN/water (1:1, v/v) and 0.1% formic acid.

The YEVGHRC peptide was purchased of Bankpeptide Biological Tech Co., LTD (Hefei, China).

2.4. Synthesis of NODAGA-YEVGHRC, NODAGA-APRPG-NH_2 and NODAGA-APRPG-COOH

2.4.1. Conjugation reaction of YEVGHRC linear peptide with Maleimide-NODAGA

9.7 mg (11 μmol) Maleimide-NODAGA was coupled to the Cys thiol-group of the linear YEVGHRC peptide (6.7 mg; 13.5 μmol). The ingredients were dissolved in a pre-deoxygenated DMF/water 3:1 solution and the pH were adjusted between 7 and 7.5. The reaction was carried out by stirring the mixtures for 2 h under He atmosphere at room temperature. The product of the reaction (NODAGA-YEVGHRC) was purified with semi-preparative RP-HPLC and then were lyophilized. The final product analysed by analytical HPLC and ESI-MS (Shimadzu LCMS IT-TOF Mass Spectrometer, Shimadzu Corp., Tokyo, Japan).

2.4.2. Conjugation reaction of APRPG-NH_2 linear peptide with p-SCN-Bn-NODAGA

5.8 mg (12 μmol) from the linear APRPG-NH_2 peptide was dissolved in 0.5 mL of DMF and 8.3 mg (14 μmol) of *p*-SCN-benzyl-NODAGA was introduced into reaction solution. Thenceforth, 4.7 μl DIPEA was added into mixture and then 50 μl water added. The reaction mixture was stirred for 24 h at room temperature. The resulting crude product (NODAGA-APRPG-NH_2) was purified on semi-preparative RP-HPLC. The pure fractions of the product were collected in a vial and then were lyophilized. The material was characterized by ESI-MS (Shimadzu LCMS IT-TOF Mass Spectrometer, Shimadzu Corp., Tokyo, Japan) and analytical RP-HPLC (as described below).

2.4.3. Conjugation reaction of APRPG-COOH linear peptide with p-SCN-Bn-NODAGA

The conjugation reaction of NODAGA-APRPG-NH_2 was identical as for NODAGA-APRPG-COOH, except that the linear peptide and amounts were different. Briefly, 10.5 mg (21 μmol) from the linear APRPG-COOH peptide was dissolved in 0.5 mL of DMF. 15.05 mg (25 μmol) of *p*-SCN-Bn-NODAGA was added into the mixture. Furthermore, 7.4 μl DIPEA was introduced into the reaction. The work-up processes were identical to the procedures described above.

2.5. RP-HPLC methods

The crude, APRPG-type peptides were purified on a KNAUER HPLC system equipped with a 2501 UV detector (H. Knauer, Bad Homburg, Germany) using a preparative Phenomenex Luna C18(2) column (100 Å, 10 μm, 250 mm × 21.2 mm) (Torrance, CA, USA). Linear gradient elution (0 min 5% B; 5 min 5% B; 50 min 50% B) with eluent A (0.1% TFA in water) and eluent B (0.1% TFA in ACN/H_2O (80:20, v/v)) was used at a flow rate of 4 mL/min. Peaks were detected at 220 nm.

Analytical RP-HPLC was performed on a KNAUER HPLC system and a 2501 UV detector using a Phenomenex Luna C18 column (100 Å, 5 μm, 250 mm × 4.6 mm) as a stationary phase. Linear gradient elution (0 min 0% B; 5 min 0% B; 50 min 90%) at a flow rate of 1 mL/min with eluents described above. Peaks were detected at 220 nm.

The chelator-conjugated peptides (NODAGA-YEVGHRC, NODAGA-APRPG-NH_2 and NODAGA-APRPG-COOH) were purified on KNAUER HPLC system using a semi-preparative Kromasil EternityXT-10-C18 column (100 Å, 10 μm, 10 × 150 mm) with a flow rate 4 mL/min. The gradient elution (0 min 10% B; 5 min 10% B; 10 min 40% B; 13 min 75% B; 20 min 75% B) in case of NODAGA-APRPG-COOH and NODAGA-APRPG-NH_2. The gradient elution was also used for the NODAGA-YEVGHRC compound (0 min 8% B; 2 min 8% B; 15 min 19% B; 20 min 50% B; 22 min 50% B). The eluent A (0.1% TFA in water) and eluent B (0.1% TFA ACN/H2O (95:5 v/v)) were used in all instances. Peaks were identified at 220 nm.

For the determination of the radiochemical purities of the radioligands, [^{68}Ga]Ga-NODAGA-YEVGHRC, [^{68}Ga]Ga-NODAGA-APRPG-NH_2 and [^{68}Ga]Ga-NODAGA-APRPG-COOH a KNAUER HPLC with a radiodetector was used. The KNAUER HPLC was equipped with a Halo C18 column (100 mm × 3 mm) 5 μm diameters, and 0.7 mL/min flow rate was applied, with a gradient profile 0 min 4% B; 2 min 4% B; 5 min 10% B; 10 min 30% B; 15 min 45% B in case of [^{68}Ga]Ga-NODAGA-APRPG-COOH and [^{68}Ga]Ga-NODAGA-APRPG-NH_2 and 0 min 0% B; 4 min 0% B; 10 min 40% B; 18 min 45% B for [^{68}Ga]Ga-NODAGA-YEVGHRC. (mobile phases are identical than mentioned earlier). Signals were detected by radiodetector and UV detector (254 nm).

2.6. Radiolabelling of NOTA-NGR, NODAGA-YEVGHRC, NODAGA-aprpg-NH_2 and NODAGA-aprpg-COOH with ^{68}Ga

Prior the determination of the protocol for the radiolabelling, optimization reactions were performed. During these experiments, the concentration of the peptides suitable to achieve a quantitative radiolabelling were discovered. Subsequently, the radiosynthesis of the NOTA-NGR, NODAGA-YEVGHRC NODAGA-APRPG-NH_2 and NODAGA-APRPG-COOH were performed manually using the allocated values. For the isotope production a fractional elution procedure was applied. The ^{68}Ge/^{68}Ga-generator was eluted with 0.1 M HCl (aq), and the 1 ml fraction of the highest activity was used for the labelling. The isotopic solution was buffered with sodium-acetate (1 M; 0.15 mL, aq.) and the pH of the mixture was adjusted to 4.0–4.1. Finally, 5 μL of 3 mM NOTA-NGR, NODAGA-YEVGHRC, NODAGA-APRPG-NH_2 or NODAGA-APRPG-COOH stock solution was introduced to the mixture and it was incubated for 5 min at 95 °C. The reaction mixture was cooled down, and the crude material was transferred to an Oasis HLB 1 cc cartridge (the column was conditioned with 400 μL of 96% EtOH and then it was rinsed with 2 mL of water). The immobilized radioactive substance was rinsed with 2 mL of water to remove the traces of the reaction media. The activity was recovered from the column with 0.2 mL of isotonic NaCl solution/EtOH 2:1 mixture, it was further diluted with saline to decrease the organic content below 10% and finally the solution was sterile filtered. [^{68}Ga]Ga-NOTA-NGR, [^{68}Ga]Ga-NODAGA-YEVGHRC, [^{68}Ga]Ga-NODAGA-APRPG-NH_2 and [^{68}Ga]Ga-NODAGA-APRPG-COOH were produced with high specific activity and with good radiochemical purity, in all cases.

2.7. Determination of partition coefficient of [^{68}Ga]Ga-NODAGA-YEVGHRC, [^{68}Ga]Ga-NODAGA-aprpg-NH_2 and [^{68}Ga]Ga-NODAGA-aprpg-COOH

The hydrophobicity of a compound is a significant feature of a radioligand, therefore the determination of it has a predictive value for the applicability of it. The partition coefficient of our new compounds was determined by measuring the activity-ratio in 1-octanol and PBS-solution (pH = 7.4). 1–2 MBq of [^{68}Ga]Ga-NODAGA-YEVGHRC, [^{68}Ga]Ga-NODAGA-APRPG-NH_2 and [^{68}Ga]Ga-NODAGA-APRPG-COOH in 10 μL aq. solution were introduced into a centrifuge tubes containing a mixture of 0.49 mL of PBS and 0.5 mL of 1-octanol. After 20 min of vigorous shaking, the tubes were centrifuged at 20.000 rpm

Table 1
Representative parameters of the newly synthetized peptide derivatives, *for the conditions see the "Material and methods" section.

Radio-peptide	Retention time (radio-peptide) (min)*	Monoisotopic mass (m/z) (calculated) peptide-precursor	(m/z) (measured) peptide-precursor
[^{68}Ga]Ga-NODAGA-YEVGHRC	12.53	1359.59	1359.66
[^{68}Ga]Ga-NODAGA-APRPG-NH_2	7.38	1016.49	1016.41
[^{68}Ga]Ga-NODAGA-APRPG-COOH	10.06	1017.47	1017.35

for 5 min for complete separation of layers. 100 μL were taken from each layer and the aliquots were transferred into test tubes; the radioactivity was measured with a PerkinElmer Packard Cobra gamma counter.

2.8. Determination of in vitro stability of [^{68}Ga]Ga-NODAGA-YEVGHRC, [^{68}Ga]Ga-NODAGA-aprpg-NH_2 and [^{68}Ga]Ga-NODAGA-aprpg-COOH

The stability of [^{68}Ga]Ga-NODAGA-YEVGHRC, [^{68}Ga]Ga-NODAGA-APRPG-NH_2 and [^{68}Ga]Ga-NODAGA-APRPG-COOH were tested in mouse serum at 37 °C. A few MBq from the radiolabelled compounds were added into a mouse serum and the mixture was incubated. In order to perform a serum stability analysis, 50 μL aliquot of [^{68}Ga]Ga-NODAGA-YEVGHRC, [^{68}Ga]Ga-NODAGA-APRPG-NH_2 and [^{68}Ga]Ga-NODAGA-APRPG-COOH at different time points (0, 30, 60, 90, 120 min) were blended with 50 μL cold abs. EtOH. The obtained precipitate was elutriated by centrifugation at 20.000 rpm for 5 min. After the collection of the supernatant and its further dilution with water, the radiochemical purity of substances was determined by the application of the analytical radio-RP-HPLC.

2.9. Cell culture method

The cell culturing method was described earlier by Kertész et al. (2017) and Trencsényi et al. (2017). Briefly, B16F10 (mouse melanoma) cells were obtained from ATCC (ATCC® CRL-6475™) and B16F10 cells were cultured in Dulbecco's Modified Eagle's medium (DMEM, GIBCO Life Technologies) supplemented with 10% Fetal Bovine Serum (FBS, Gibco Life technologies), 1% MEM Vitamins solution (Sigma-Aldrich), 1% (v/v) MEM Non Essential Amino Acid solution (Sigma-Aldrich), and 1% Antibiotic and Antimycotic solution (Sigma-Aldrich). B16F10 cells were maintained in T75 flasks (Sarstedt Ltd.) at 37 °C and 5% CO_2 tension. For tumor induction B16F10 cells were used after five passages, and the cell viability was higher than 90% which was verified by tripan blue exclusion test.

2.10. Animal housing

12 weeks old male C57BL/6 mice (n = 60) were used for *in vivo* animal studies. Animals were purchased from Animalab Ltd. (Distributor of The Jackson Laboratory, USA). The animals were housed under conventional conditions (26 ± 2 °C and 55 ± 10% humidity) with the ad libitum accessibility of tap water and VRF-1 rodent diet (Special Diets Services, Akronom Ltd.). The animal experiments were authorized by the Ethical Committee for Animal Research, University of Debrecen, Hungary (permission number: 8/2016/DEMÁB). Laboratory animals were kept according to the Hungarian Laws and animal welfare directions and regulations of the European Union.

2.11. Animal model

The C57BL/6 mice were anaesthetized with 3% Isoflurane (Forane) using a preclinical anaesthesia device (Eickemeyer, Tec3 Isoflurane Vaporizer), and after depilation of the area of left shoulder, 5×10^6 B16F10 cells were inoculated subcutaneously in 150 μL sterile saline.

2.12. In vivo animal study and quantitative PET analysis

8–9 days after B16F10 tumor induction, tumor-bearing (n = 40) and healthy, control (n = 20) animals were anaesthetized by 3% Isoflurane, and 5.5 ± 0.7 MBq of [^{68}Ga]Ga-NOTA-cNGR or [^{68}Ga]Ga-NODAGA-YEVGHRC or [^{68}Ga]Ga-NODAGA-APRPG-NH_2 or [^{68}Ga]Ga-NODAGA-APRPG-COOH was injected via the lateral tail vein. After 90 min uptake time, the animals were anaesthetized, and static PET scans (t = 20 min) were performed using the preclinical small animal MiniPET-II scanner. The 3D reconstructed images were evaluated with BrainCAD image analysis software. The subcutaneous B16F10 tumor and muscle (as background) areas were manually drawn round to determine the VOI

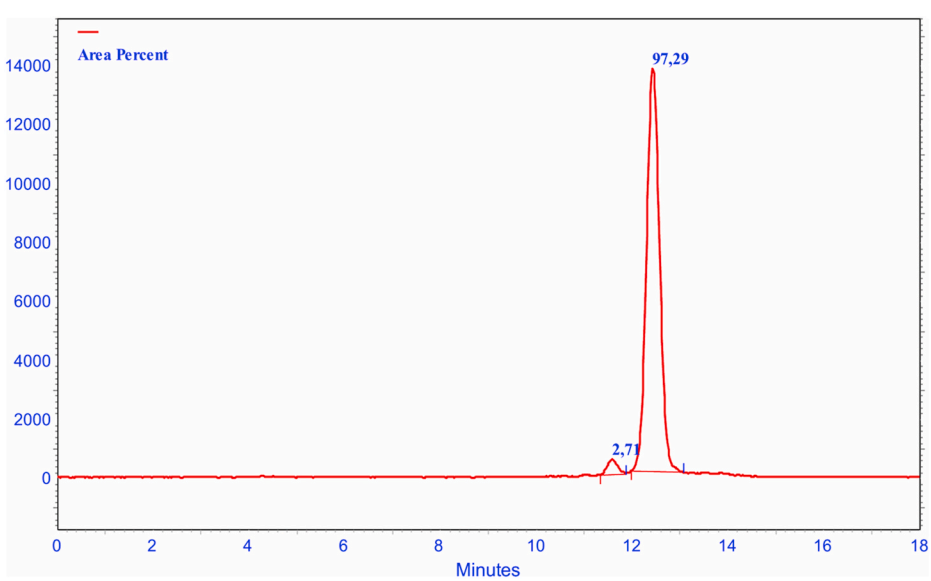

Fig. 1. RP-HPLC of [^{68}Ga]Ga-NODAGA-YEVGHRC

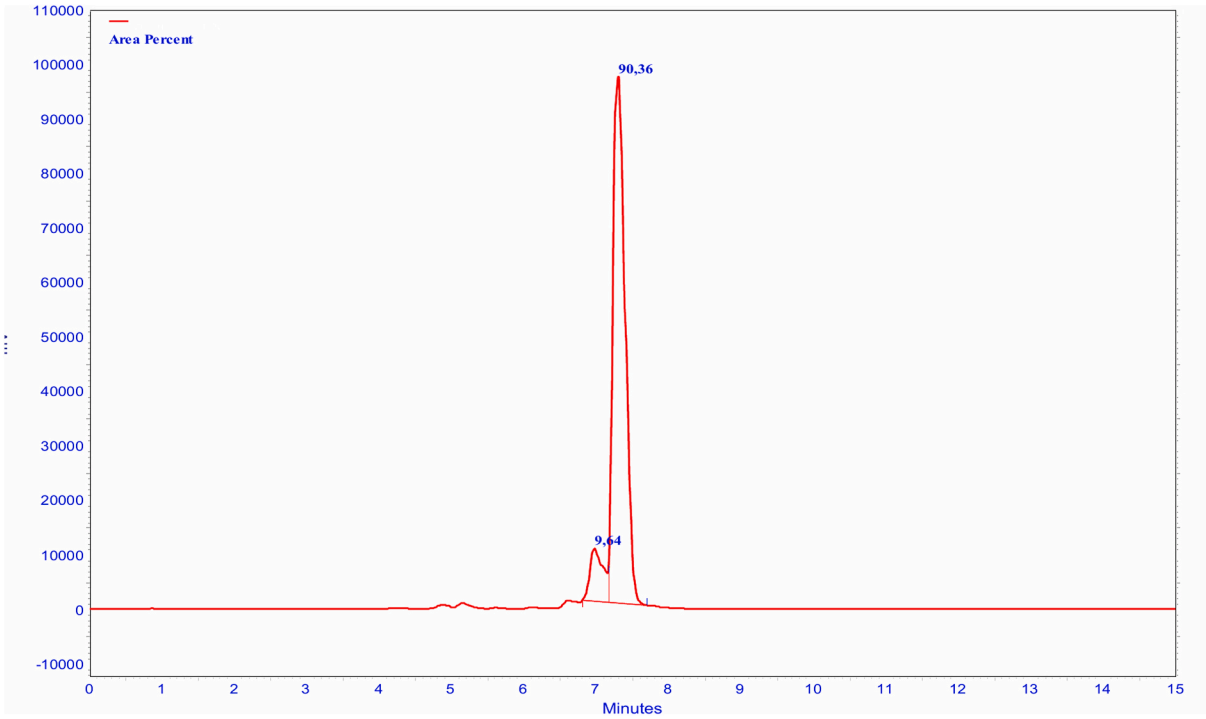

Fig. 2. RP-HPLC of [^{68}Ga]Ga-NODAGA-APRPG-NH_2.

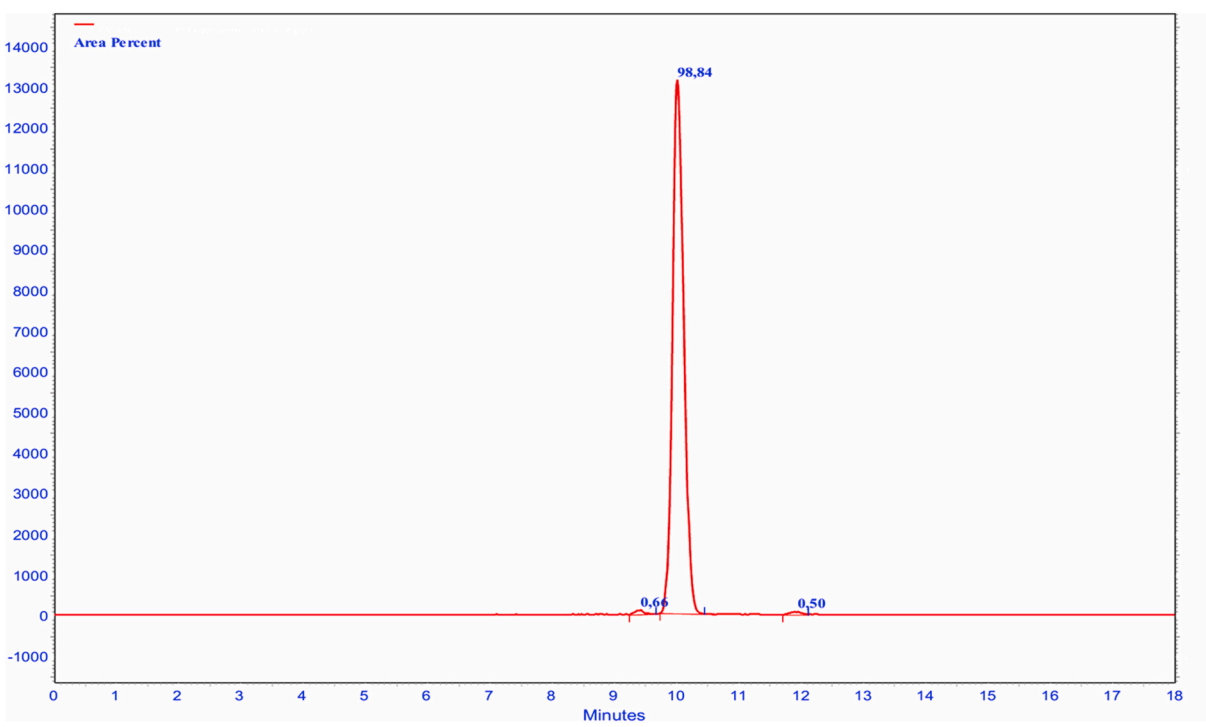

Fig. 3. RP-HPLC of [^{68}Ga]Ga-NODAGA-APRPG-COOH.

(volume of interest) of these tissues. The radiotracer uptake was defined in SUV (standardized uptake value) value.

2.13. *Ex vivo animal study*

After *in vivo* PET imaging animals were euthanized with 5% isoflurane. For the determination of the biodistribution of [^{68}Ga]Ga-NOTA-cNGR, [^{68}Ga]Ga-NODAGA-YEVGHRC, [^{68}Ga]Ga-NODAGA-APRPG-NH_2 and [^{68}Ga]Ga-NODAGA-APRPG-COOH blood and urine were collected and small tissue samples were taken from liver, spleen, kidneys, small- and large intestine, stomach, muscle, fat and B16F10 tumor. The weight of the samples was measured and the radioactivity was determined by a gamma-counter (PerkinElmer Packard Cobra, Waltham, MA, USA). The radiotracer uptake was expressed as %ID/g.

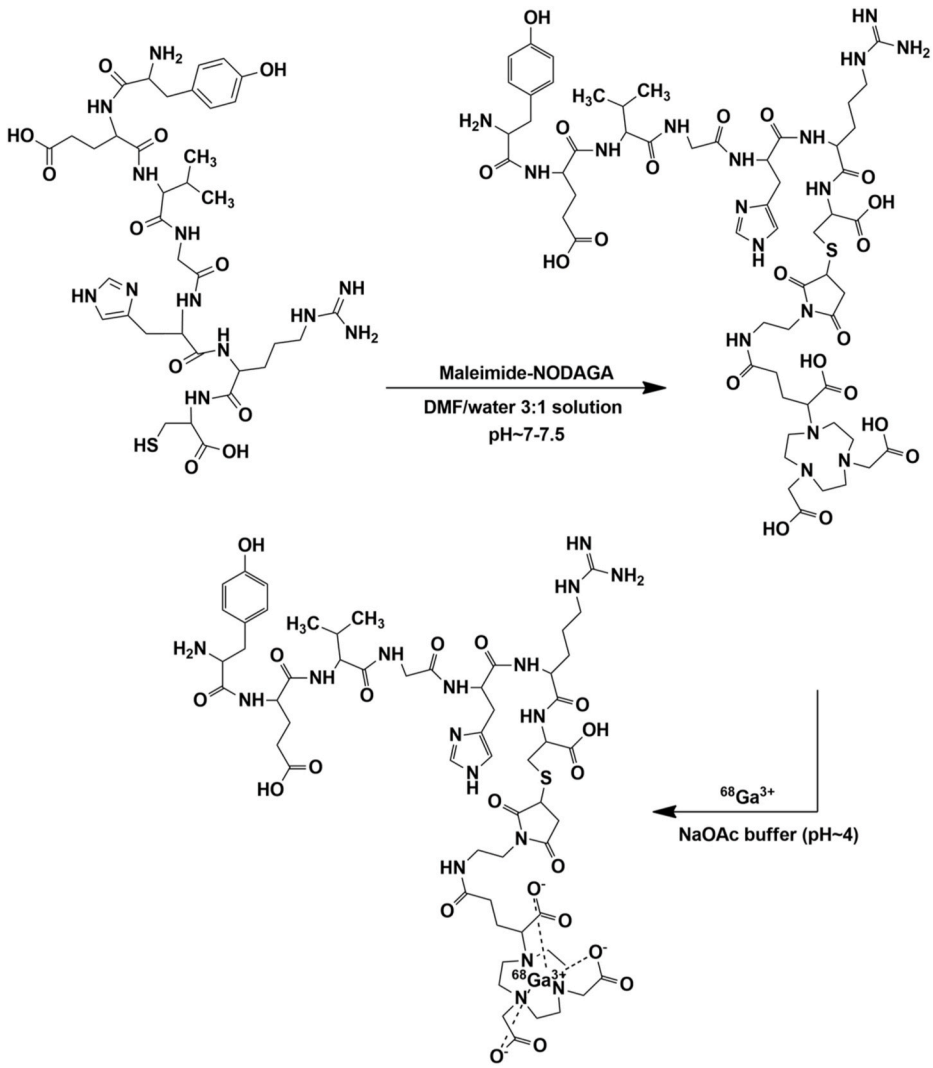

Fig. 4. Conjugation and radiolabelling of YEVGHRC peptide.

2.14. Statistical analysis

Experimental data was presented as mean ± SD of at least three independent experiments. The significance was calculated by two-tailed Student's t-test, and two-way ANOVA test. The significance level was $p \leq 0.05$, unless otherwise indicated.

3. Results and discussion

3.1. Chemical and radiochemical synthesis

The APRPG-COOH peptide was prepared on 2-ClTrt resin by SPPS using standard Fmoc-chemistry. The APRPG-NH_2 peptide was synthesized on Rink-Amide MBHA. The crude peptides were purified by RP-HPLC, and the isolated yields of the end products were over 70%. The purity of the carrier peptides APRPG-NH_2, APRPG-COOH were assessed with analytical HPLC (the retention times of the pure peptides were t_R = 13.7 min of APRPG-COOH; t_R = 12.9 min of APRPG-NH_2) and proved to be ≥ 99%. The chemical identity of the peptides were assessed by MS and the molecular mass was found to be $[M+H]^{2+} = 249.1$ and $[M+H]^{+} = 497.3$ for APRPG-COOH and $[M+H]^{2+} = 248.7$ and $[M+H]^{+} = 493.3$ for APRPG-NH_2 respectively.

The free amino group on the alanine moiety of APRPG peptides were reacted with *p*-SCN-benzyl-NODAGA chelator. The complete ligands were purified with RP-HPLC and then were lyophilized. The YEVGHRC analogue was decorated with the chelator on the side chain of the Cys, forming a thioether bond with the maleimide moiety. The chemical identity – assessed by MS - of the precursor peptides and the HPLC properties of the applied radioligands are summarized in Table 1.

The labelling protocols of all peptide-derivates were manual procedures and the overall synthesis time was 25 min all cases including the cleaning and the formulation step also. The decay corrected yield was in the range 67–73% (n = 12) and the radiochemical purity was better than 95% except the [^{68}Ga]Ga-NODAGA-APRPG-NH_2, where the purity exceeds the 90% (Figs. 1–3). The specific activity was 14.87 ± 0.13 GBq/μmol for [^{68}Ga]Ga-NODAGA-YEVGHRC, 15.40 ± 0.09 GBq/μmol for [^{68}Ga]Ga-NODAGA-APRPG-NH_2 and 19.47 ± 0.12 GBq/μmol for [^{68}Ga]Ga-NODAGA-APRPG-COOH. The chemical structures of the newly synthesized peptides can be seen in Fig. 4 and Fig. 5.

3.2. Partition coefficient and in vitro stability of all radiolabelled peptide-derivates

The partition coefficients (log*P*) were determined for the three, newly synthetized radiotracers, thus log*P* of [^{68}Ga]Ga-NODAGA-YEVGHRC proved to be −4.421, [^{68}Ga]Ga-NODAGA-APRPG-NH_2 was −3.024 and [^{68}Ga]Ga-NODAGA-APRPG-COOH resulted in −2.370, proposing that these radiopharmaceuticals are highly hydrophilic. Moreover, the stability of the labelled substances in rat and mouse serum at 37 °C was investigated, by means of an analytical radio-HPLC. After 2

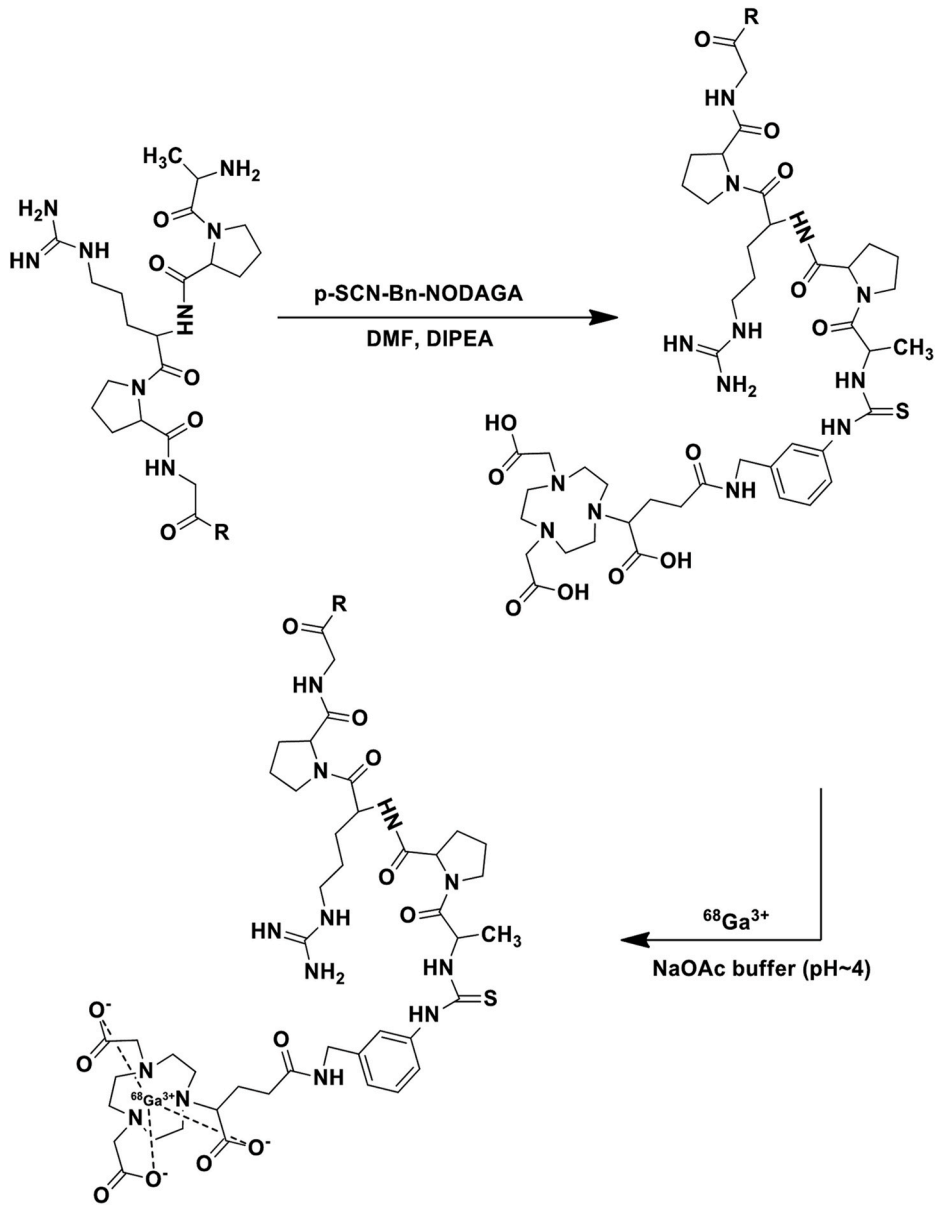

Fig. 5. Conjugation and radiolabelling of APRPG peptides R = OH [^{68}Ga]Ga-NODAGA-APRPG-COOH; R = NH_2 [^{68}Ga]Ga-NODAGA-APRPG-NH_2.

h of incubation in serum, more than 80% of the original labelled peptides were found intact, in all cases.

3.3. *In vivo and ex vivo biodistribution studies on healthy animals*

For the determination of the biodistribution of the newly synthesized APN/CD13 specific [^{68}Ga]Ga-NODAGA-YEVGHRC, and the VEGFR-1 specific [^{68}Ga]Ga-NODAGA-APRPG-NH_2 and [^{68}Ga]Ga-NODAGA-APRPG-COOH probes, *in vivo* and *ex vivo* studies were carried out using healthy control C57BL/6 mice. After the qualitative analysis of the decay-corrected PET images it was found that the kidneys showed high accumulation 90 min post injection of [^{68}Ga]Ga-NOTA-cNGR, [^{68}Ga]Ga-NODAGA-YEVGHRC, [^{68}Ga]Ga-NODAGA-APRPG-NH_2 and [^{68}Ga]Ga-NODAGA-APRPG-COOH which was applied as a reference compound (Fig. 6). In previous studies of our research group, we also found that the ^{68}Ga-labelled APN/CD13 specific peptides ([^{68}Ga]Ga-NOTA-cNGR, [^{68}Ga]Ga-NODAGA-cNGR, [^{68}Ga]Ga-NODAGA-cNGR (MG1) or [^{68}Ga]Ga-NODAGA-cNGR (MG2)) are excreted through the urinary system of the animals due to their highly hydrophilic properties, which was confirmed by the log*P* values (Kis et al., 2020a; Máté et al., 2015). However, there was a significant difference between the log*P* values of the newly synthesized radiopharmaceuticals. The [^{68}Ga]Ga-NODAGA-APRPG-COOH molecule was less hydrophilic (log*P*: 2.37), which was also confirmed by *ex vivo* biodistribution studies. Significantly (at $p \leq 0.05$ and $p \leq 0.01$) higher %ID/g tissue values were observed in the blood, spleen, stomach, lung, heart, and fat after the injection of [^{68}Ga]Ga-NODAGA-APRPG-COOH, than that of the three other investigated radiotracers (Fig. 6E). Due to its less hydrophilic property, it remains in the circulation for longer time resulting a higher background radioactivity. Between the %ID/g values of [^{68}Ga]Ga-NOTA-cNGR, [^{68}Ga]Ga-NODAGA-YEVGHRC, and [^{68}Ga]Ga-NODAGA-APRPG-NH_2 we found no significant difference (at $p \leq 0.05$) in any of the organs and tissues examined.

3.4. *In vivo and ex vivo comparative studies on subcutaneous tumor model*

For the assessment of the APN/CD13 specificity of the [^{68}Ga]Ga-NOTA-c(NGR) and [^{68}Ga]Ga-NODAGA-YEVGHRC, and the VEGFR-1 specificity of [^{68}Ga]Ga-NODAGA-APRPG-NH_2 and [^{68}Ga]Ga-NODAGA-

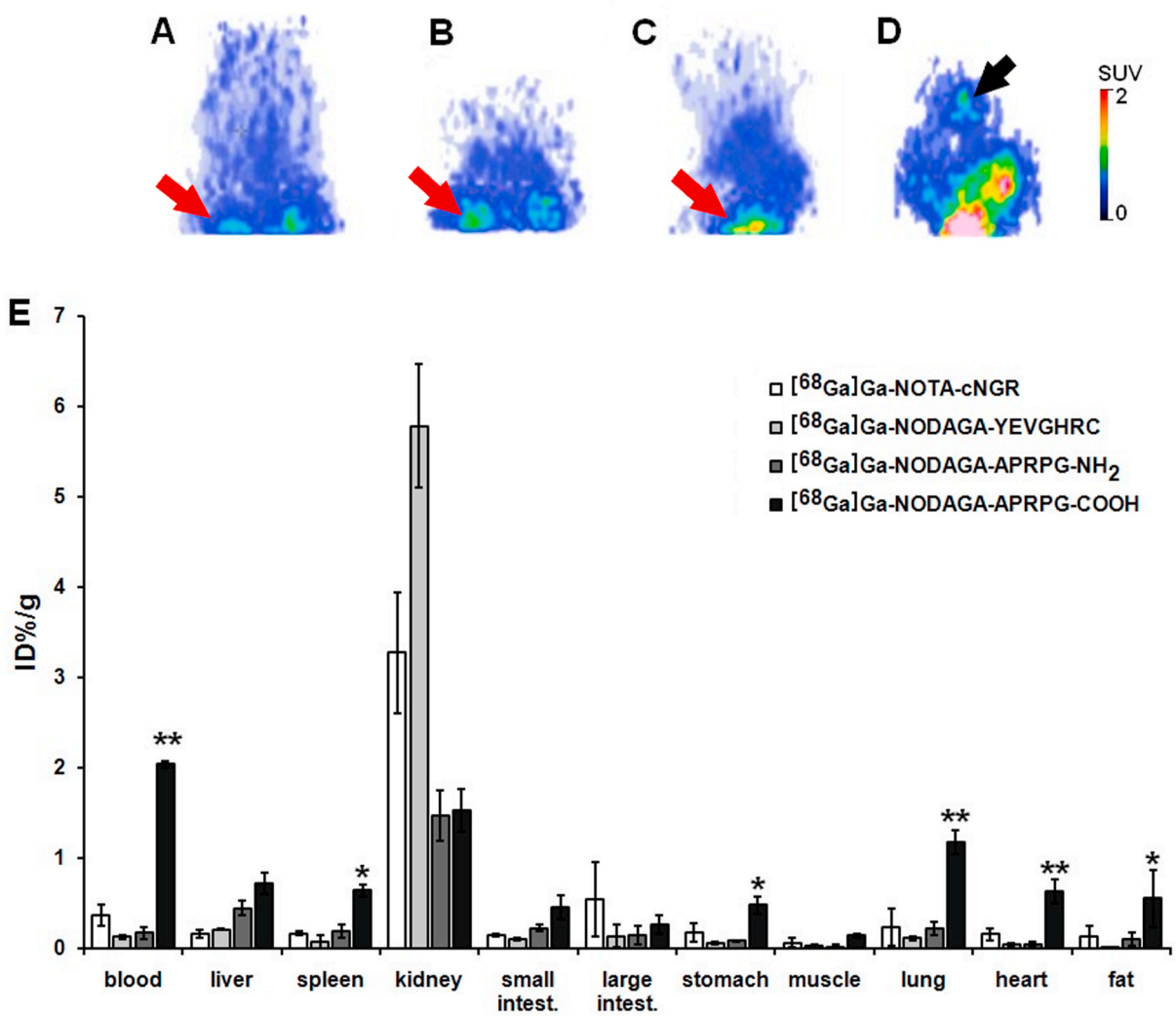

Fig. 6. *In vivo* PET imaging and *ex vivo* biodistribution data for [^{68}Ga]Ga-NOTA-c(NGR), [^{68}Ga]Ga-NODAGA-YEVGHRC, [^{68}Ga]Ga-NODAGA-APRPG-NH_2 and [^{68}Ga]Ga-NODAGA-APRPG-COOH. Representative decay-corrected coronal PET images of healthy control C57BL/6 mice 90 min after intravenous injection of [^{68}Ga]Ga-NOTA-c(NGR) (A), [^{68}Ga]Ga-NODAGA-YEVGHRC (B), [^{68}Ga]Ga-NODAGA-APRPG-NH_2 (C) and [^{68}Ga]Ga-NODAGA-APRPG-COOH (D). Black arrow: liver; red arrows: kidney. E: quantitative analysis of *ex vivo* biodistribution data (n = 5 healthy control mice/radiotracer) 90 min after tracer injection %ID/g values are presented as mean ± SD. Significance levels: $p \leq 0.05$ (*) and $p \leq 0.01$ (**). (For interpretation of the references to colour in this figure legend, the reader is referred to the Web version of this article.)

APRPG-COOH probes, *in vivo* and *ex vivo* comparative studies were performed on B16F10 tumor-bearing mice. Previous studies have demonstrated that B16F10 tumor cells showed APN/CD13 and VEGFR-1 positivity by molecular biological methods and PET imaging (Graziani et al., 2016; Guzman-Rojas et al., 2012; Satpati et al., 2017). Our *in vivo* PET imaging results correlated well with these findings where the B16F10 tumors were clearly visualized by our tumor-associated neo--angiogenic marker specific ^{68}Ga-labelled radiopharmaceuticals. However, among the investigated radiopharmaceuticals the APN/CD13 specific [^{68}Ga]Ga-NOTA-c(NGR) and the VEGFR-1 receptor-specific [^{68}Ga]Ga-NODAGA-APRPG-COOH showed the highest accumulation in the subcutaneously growing B16F10 tumors (Fig. 7A–D). After the quantitative SUV analysis of the decay-corrected PET images we found significantly ($p \leq 0.01$) lower uptake in the B16F10 tumors after the injection of the APN/CD13 specific [^{68}Ga]Ga-NODAGA-YEVGHRC (SUVmean: 0.03 ± 0.01) and the VEGFR-1 specific [^{68}Ga]Ga-NODAGA-APRPG-NH_2 (SUVmean: 0.04 ± 0.003) than that of APN/CD13 specific [^{68}Ga]Ga-NOTA-cNGR and the VEGFR-1 specific [^{68}Ga]Ga-NODAGA-APRPG-COOH, where the SUVmean values were 0.12 ± 0.02 and 0.10 ± 0.01, respectively (Fig. 7E). Interestingly, previous studies (Jia et al., 2017) have shown that YEVGHRC peptide-functionalized liposomes effectively targeted the APN-CD13-positive tumors. In our study, the radiolabelled YEVGHRC did not show sufficient targeting properties. These *in vivo* results correlated well with the *ex vivo* findings where we also find remarkable [^{68}Ga]Ga-NOTA-cNGR (%ID/g: 1.60 ± 0.30) and [^{68}Ga]Ga-NODAGA-APRPG-COOH (%ID/g: 1.35 ± 0.11) uptake in the B16F10 tumors. Significantly lower accumulation was observed in the tumors after the injection of [^{68}Ga]Ga-NODAGA-YEVGHRC (%ID/g: 0.13 ± 0.06) and [^{68}Ga]Ga-NODAGA-APRPG-NH_2 SUVmean: (%ID/g: 0.23 ± 0.05) (Fig. 7F). Similar results were found when the APN/CD13 specificity of ^{68}Ga-labelled different NGR derivatives were investigated using hepatocellular carcinoma, mesoblastic nephroma and melanoma tumorous models (Kis et al., 2020a, 2020bbib_Kis_et_al_2020_7bib_Kis_et_al_2020b; Máté et al., 2015; Satpati et al., 2017). Among the several NGR forms the ^{68}Ga-labelled cyclic NGR (KNGRE) showed the best tumor targeting properties.

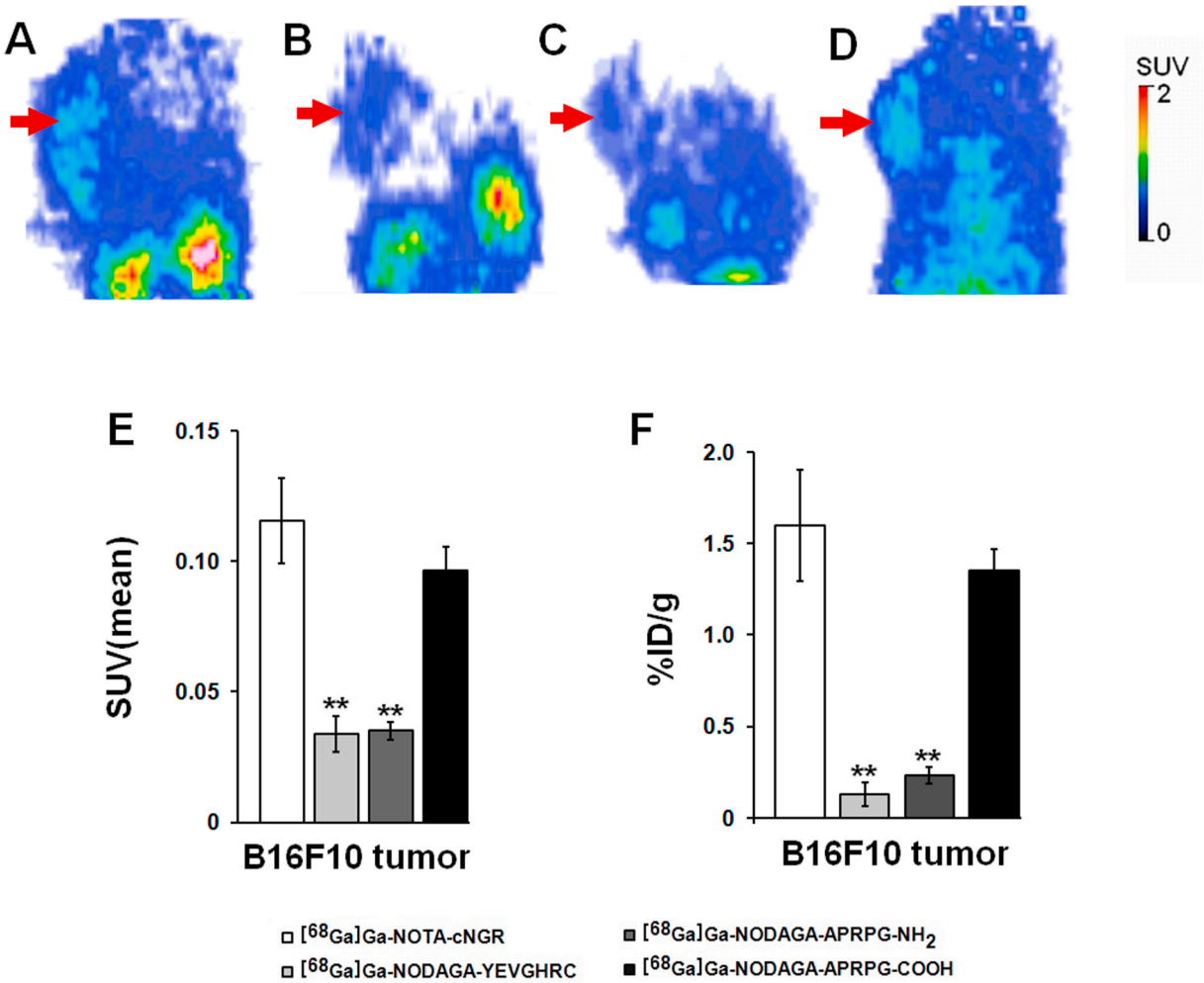

Fig. 7. *In vivo* PET imaging and *ex vivo* biodistribution data for [^{68}Ga]Ga-NOTA-c(NGR), [^{68}Ga]Ga-NODAGA-YEVGHRC, [^{68}Ga]Ga-NODAGA-APRPG-NH_2 and [^{68}Ga]Ga-NODAGA-APRPG-COOH. Representative decay-corrected coronal PET images of B16F10 tumor-bearing C57BL/6 mice 90 min after intravenous injection of [^{68}Ga]Ga-NOTA-c(NGR) (A), [^{68}Ga]Ga-NODAGA-YEVGHRC (B), [^{68}Ga]Ga-NODAGA-APRPG-NH_2 (C) and [^{68}Ga]Ga-NODAGA-APRPG-COOH (D). Red arrows: subcutaneous B16F10 tumor. Quantitative SUV (E) and %ID/g (F) analysis of biodistribution data (n = 10 B16F10 tumor/radiotracer) 90 min after tracer injection. SUV and %ID/g values are presented as mean ± SD. Significance level: $p \leq 0.01$ (**). (For interpretation of the references to colour in this figure legend, the reader is referred to the Web version of this article.)

4. Conclusion

Among markers of tumor neo-angiogenesis, APN/CD13 is a very promising target in positron emission tomography imaging, however, the selection of the appropriate ^{68}Ga-labelled NGR-based radiopharmaceutical (*e.g.*: [^{68}Ga]Ga-NOTA- and NODAGA-c(NGR) with the highest binding affinity in this study) is critical for the precise detection of tumors neo-angiogenesis and for monitoring the efficacy of anticancer therapy. But the NGR motif is prone to non-enzymatic deamidation through succinimide ring formation followed by hydrolysis (Curnis et al., 2006), therefore it could be essential to find new sequences with improved chemical stability to create the ideal radiopharmaceutical for the detection of neo-angiogenesis. In this work we examined new, non-NGR linear analogues to visualize angiogenesis with non-vulnerable amino acid sequences to evaluate the potency in them. Despite the APRPG and YEVGHRC are not optimized vectors yet, but we have found specific accumulation of the radioligands in the animal model. From the newly developed radioligands [^{68}Ga]Ga-NODAGA-APRPG-COOH showed comparable parameters on the B16F10 tumor-model than the reference compound [^{68}Ga]Ga-NOTA-c(NGR), and can be a promising candidate for further development.

Credit author statement

Noémi Dénes: Writing – original draft, methodology, Adrienn Kis: Methodology, Judit P. Szabó: Animal handling, István Jószai: HPLC analysis, István Hajdu: Radiolabelling, Viktória Arató: *In vivo* experiments, Kata Nóra Enyedi: Peptide synthesis, Gábor Mező: Methodology, János Hunyadi: Funding acquisition, György Trencsényi: Writing – review & editing, István Kertész: Writing – review & editing.

Declaration of competing interest

The authors declare that they have no known competing financial interests or personal relationships that could have appeared to influence the work reported in this paper.

Acknowledgements

The contribution of the first author to this research project was supported by Ministry for Innovation and Technology, managed by the National Research, Development and Innovation Office in the framework of ÚNKP-19-3-I-DE-195 'New National Excellence Programme'. This work was also supported by the Thematic Excellence Programme of

the Ministry for Innovation and Technology in Hungary (ED_18-1-2019-0028), within the framework of the Space Sciences thematic programme of the University of Debrecen. This research was also supported by the National Research, Development and Innovation Office under grant NKFIH K119552 and NVKP_16-1-2016-0036, and by EFOP-3.6.3-VEKOP-16-2017-00009 co-financed by EU and the European Social Found. The research was supported also by the Thematic Excellence Programme (TKP2020-NKA-04) of the Ministry for Innovation and Technology in Hungary.

References

Arap, W., Pasqualini, R., Ruoslahti, E., 1998 Jan 16. Cancer treatment by targeted drug delivery to tumor vasculature in a mouse model. Science 279 (5349), 377–380. https://doi.org/10.1126/science.279.5349.377. PMID: 9430587.

Banerjee, S.R., Pomper, M.G., 2013 Jun. Clinical applications of gallium-68. Appl. Radiat. Isot. 76, 2–13. https://doi.org/10.1016/j.apradiso.2013.01.039. Epub 2013 Feb 20. PMID: 23522791; PMCID: PMC3664132.

Chen, K., Ma, W., Li, G., Wang, J., Yang, W., Yap, L.P., Hughes, L.D., Park, R., Conti, P.S., 2013 Jan 7. Synthesis and evaluation of 64Cu-labeled monomeric and dimeric NGR peptides for MicroPET imaging of CD13 receptor expression. Mol. Pharm. 10 (1), 417–427. https://doi.org/10.1021/mp3005676. Epub 2012 Dec 13. PMID: 23190134.

Colombo, G., Curnis, F., De Mori, G.M., Gasparri, A., Longoni, C., Sacchi, A., Longhi, R., Corti, A., 2002 Dec 6. Structure-activity relationships of linear and cyclic peptides containing the NGR tumor-homing motif. J. Biol. Chem. 277 (49), 47891–47897. https://doi.org/10.1074/jbc.M207500200. Epub 2002 Oct 7. PMID: 12372830.

Curnis, F., Longhi, R., Crippa, L., Cattaneo, A., Dondossola, E., Bachi, A., Corti, A., 2006 Nov 24. Spontaneous formation of L-isoaspartate and gain of function in fibronectin. J. Biol. Chem. 281 (47), 36466–36476. https://doi.org/10.1074/jbc.M604812200. Epub 2006 Oct 2. PMID: 17015452.

Denekamp, J., 1993 Mar. Review article: angiogenesis, neovascular proliferation and vascular pathophysiology as targets for cancer therapy. Br. J. Radiol. 66 (783), 181–196. https://doi.org/10.1259/0007-1285-66-783-181. PMID: 7682469.

Ellis, L.M., Ahmad, S., Fan, F., Liu, W., Jung, Y.D., Stoeltzing, O., Reinmuth, N., Parikh, A.A., 2002 Apr. Angiopoietins and their role in colon cancer angiogenesis. Oncology (Williston Park) 16 (4 Suppl. 3), 31–35. PMID: 12014866.

Ellis, L.M., Liu, W., Ahmad, S.A., Fan, F., Jung, Y.D., Shaheen, R.M., Reinmuth, N., 2001 Oct. Overview of angiogenesis: biologic implications for antiangiogenic therapy. Semin. Oncol. 28 (5 Suppl. 16), 94–104. https://doi.org/10.1016/s0093-7754(01)90287-8. PMID: 11706401.

Folkman, J., 1971 Nov 18. Tumor angiogenesis: therapeutic implications. N. Engl. J. Med. 285 (21), 1182–1186. https://doi.org/10.1056/NEJM197111182852108. PMID: 4938153.

Graziani, G., Ruffini, F., Tentori, L., Scimeca, M., Dorio, A.S., Atzori, M.G., Failla, C.M., Morea, V., Bonanno, E., D'Atri, S., Lacal, P.M., 2016 Nov 8. Antitumor activity of a novel anti-vascular endothelial growth factor receptor-1 monoclonal antibody that does not interfere with ligand binding. Oncotarget 7 (45), 72868–72885. https://doi.org/10.18632/oncotarget.12108. PMID: 27655684; PMCID: PMC5341950.

Guzman-Rojas, L., Rangel, R., Salameh, A., Edwards, J.K., Dondossola, E., Kim, Y.G., Saghatelian, A., Giordano, R.J., Kolonin, M.G., Staquicini, F.I., Koivunen, E., Sidman, R.L., Arap, W., Pasqualini, R., 2012 Jan 31. Cooperative effects of aminopeptidase N (CD13) expressed by nonmalignant and cancer cells within the tumor microenvironment. Proc. Natl. Acad. Sci. U. S. A. 109 (5), 1637–1642. https://doi.org/10.1073/pnas.1120790109. Epub 2012 Jan 17. PMID: 22307623; PMCID: PMC3277167.

Jia, X., Han, Q., Wang, Z., Qian, Y., Jia, Y., Wang, W., Hu, Z., 2017 Feb 28. Targeting peptide functionalized liposomes towards aminopeptidase N for precise tumor diagnosis and therapy. Biomater. Sci. 5 (3), 417–421. https://doi.org/10.1039/c6bm00898d. PMID: 28138675.

Kazerounian, S., Lawler, J., 2018 Mar. Integration of pro- and anti-angiogenic signals by endothelial cells. J. Cell Commun. Sig. 12 (1), 171–179. https://doi.org/10.1007/s12079-017-0433-3. Epub 2017 Dec 20. PMID: 29264709; PMCID: PMC5842194.

Kertész, István, Vida, András, Nagy, Gábor, Emri, Miklós, Farkas, Antal, Kis, Adrienn, Angyal, János, Dénes, Noémi, Szabó, Judit P., Kovács, Tünde, Bai, Péter, Trencsényi, György, 2017. *In vivo* imaging of experimental melanoma tumors using the novel radiotracer ^{68}Ga-NODAGA-Procainamide (PCA). J. Canc. 8 (5), 774–785. https://doi.org/10.7150/jca.17550.

Kirikoshi, R., Manabe, N., Takahashi, O., 2017 Feb 16. Succinimide formation from an NGR-containing cyclic peptide: computational evidence for catalytic roles of phosphate buffer and the arginine side chain. Int. J. Mol. Sci. 18 (2), 429. https://doi.org/10.3390/ijms18020429. PMID: 28212316; PMCID: PMC5343963.

Kis, A., Szabó, J.P., Dénes, N., Vágner, A., Nagy, G., Garai, I., Fekete, A., Szikra, D., Hajdu, I., Matolay, O., Méhes, G., Mező, G., Kertész, I., Trencsényi, G., 2020. In *Vivo* imaging of hypoxia and neoangiogenesis in experimental syngeneic hepatocellular carcinoma tumor model using positron emission tomography. BioMed Res. Int., 4952372 https://doi.org/10.1155/2020/4952372. PMID: 32832549; PMCID: PMC7428931.

Li, G., Wang, X., Zong, S., Wang, J., Conti, P.S., Chen, K., 2014 Nov 3. MicroPET imaging of CD13 expression using a (64)Cu-labeled dimeric NGR peptide based on sarcophagine cage. Mol. Pharm. 11 (11), 3938–3946. https://doi.org/10.1021/mp500354x. Epub 2014 Jul 30. PMID: 25054774.

Luan, Y., Xu, W., 2007. The structure and main functions of aminopeptidase N. Curr. Med. Chem. 14 (6), 639–647. https://doi.org/10.2174/092986707780059571. PMID: 17346152.

99m Ma, W., Kang, F., Wang, Z., Yang, W., Li, G., Ma, X., Li, G., Chen, K., Zhang, Y., Wang, J., 2013 May. Tc-labeled monomeric and dimeric NGR peptides for SPECT imaging of CD13 receptor in tumor-bearing mice. Amino Acids 44 (5), 1337–1345. https://doi.org/10.1007/s00726-013-1469-1. Epub 2013 Mar 1. PMID: 23456486.

Máté, G., Kertész, I., Enyedi, K.N., Mező, G., Angyal, J., Vasas, N., Kis, A., É, Szabó, Emri, M., Bíró, T., Galuska, L., Trencsényi, G., 2015 Mar 10. In vivo imaging of Aminopeptidase N (CD13) receptors in experimental renal tumors using the novel radiotracer (68)Ga-NOTA-c(NGR). Eur. J. Pharmaceut. Sci. 69, 61–71. https://doi.org/10.1016/j.ejps.2015.01.002. Epub 2015 Jan 13. PMID: 25592229.

Meinwald, Y.C., Stimson, E.R., Scheraga, H.A., 1986 Jul. Deamidation of the asparaginyl-glycyl sequence. Int. J. Pept. Protein Res. 28 (1), 79–84. https://doi.org/10.1111/j.1399-3011.1986.tb03231.x. Erratum in: Int J Pept Protein Res 1986 Dec;28(6): following 660. PMID: 3759344.

Nishida, N., Yano, H., Nishida, T., Kamura, T., Kojiro, M., 2006. Angiogenesis in cancer. Vasc. Health Risk Manag. 2 (3), 213–219. https://doi.org/10.2147/vhrm.2006.2.3.213. PMID: 17326328; PMCID: PMC1993983.

Oku, N., Asai, T., Watanabe, K., Kuromi, K., Nagatsuka, M., Kurohane, K., Kikkawa, H., Ogino, K., Tanaka, M., Ishikawa, D., Tsukada, H., Momose, M., Nakayama, J., Taki, T., 2002 Apr 18. Anti-neovascular therapy using novel peptides homing to angiogenic vessels. Oncogene 21 (17), 2662–2669. https://doi.org/10.1038/sj.onc.1205347. PMID: 11965539.

Pasqualini, R., Koivunen, E., Kain, R., Lahdenranta, J., Sakamoto, M., Stryhn, A., Ashmun, R.A., Shapiro, L.H., Arap, W., Ruoslahti, E., 2000 Feb 1. Aminopeptidase N is a receptor for tumor-homing peptides and a target for inhibiting angiogenesis. Canc. Res. 60 (3), 722–727. PMID: 10676659; PMCID: PMC4469333.

Satpati, D., Sharma, R., Kumar, C., Sarma, H.D., Dash, A., 2017 Feb 16. ^{68}Ga-Chelation and comparative evaluation of *N,N'*-bis-[2-hydroxy-5-(carboxyethyl)benzyl] ethylenediamine-*N,N'*-diacetic acid (HBED-CC) conjugated NGR and RGD peptides as tumor targeted molecular imaging probes. Med. Chem. Comm. 8 (3), 673–679. https://doi.org/10.1039/c7md00006e. PMID: 30108785; PMCID: PMC6071919.

Satpati, D., Sharma, R., Sarma, H.D., Dash, A., 2018 Mar. Comparative evaluation of ^{68}Ga-labeled NODAGA, DOTAGA, and HBED-CC-conjugated cNGR peptide chelates as tumor-targeted molecular imaging probes. Chem. Biol. Drug Des. 91 (3), 781–788. https://doi.org/10.1111/cbdd.13143. Epub 2017 Dec 6. PMID: 29130625.

Shao, Y., Liang, W., Kang, F., Yang, W., Ma, X., Li, G., Zong, S., Chen, K., Wang, J., 2014 Aug 5. 68Ga-labeled cyclic NGR peptide for microPET imaging of CD13 receptor expression. Molecules 19 (8), 11600–11612. https://doi.org/10.3390/molecules190811600. PMID: 25100253; PMCID: PMC6271277.

Simons, M., 2005 Mar 29. Angiogenesis: where do we stand now? Circulation 111 (12), 1556–1566. https://doi.org/10.1161/01.CIR.0000159345.00591.8F. PMID: 15795364.

Smith, D.L., Breeman, W.A., Sims-Mourtada, J., 2013 Jun. The untapped potential of Gallium 68-PET: the next wave of ^{68}Ga-agents. Appl. Radiat. Isot. 76, 14–23. https://doi.org/10.1016/j.apradiso.2012.10.014. Epub 2012 Oct 29. PMID: 23232184.

Trencsényi, György, Dénes, Noémi, Nagy, Gábor, Kis, Adrienn, Vida, András, Farkas, Flóra, Szabó, Judit P., Kovács, Tünde, Berényi, Ervin, Garai, Ildikó, Bai, Péter, Hunyadi, János, Kertész, István, 2017. Comparative preclinical evaluation of ^{68} Ga-NODAGA and ^{68} Ga-HBED-CC conjugated procainamide in melanoma imaging. J. Pharm. Biomed. Anal. 139, 54–64. https://doi.org/10.1016/j.jpba.2017.02.049.

van Hensbergen, Y., Broxterman, H.J., Rana, S., van Diest, P.J., Duyndam, M.C., Hoekman, K., Pinedo, H.M., Boven, E., 2004 Feb 1. Reduced growth, increased vascular area, and reduced response to cisplatin in CD13-overexpressing human ovarian cancer xenografts. Clin. Canc. Res. 10 (3), 1180–1191. https://doi.org/10.1158/1078-0432.ccr-0482-3. PMID: 14871998.

Velikyan, I., 2013 Dec 10. Prospective of ^{68}Ga-radiopharmaceutical development. Theranostics 4 (1), 47–80. https://doi.org/10.7150/thno.7447. PMID: 24396515; PMCID: PMC3881227.

von Wallbrunn, A., Waldeck, J., Höltke, C., Zühlsdorf, M., Mesters, R., Heindel, W., Schäfers, M., Bremer, C., 2008 Jan-Feb. In vivo optical imaging of CD13/APN-expression in tumor xenografts. J. Biomed. Opt. 13 (1), 011007 https://doi.org/10.1117/1.2839046. PMID: 18315356.

Wang, R.E., Niu, Y., Wu, H., Amin, M.N., Cai, J., 2011. Development of NGR peptide-based agents for tumor imaging. Am. J. Nucl. Med. Mol. Imag. 1 (1), 36–46. Epub 2011 Jul 3. PMID: 23133793; PMCID: PMC3477716.

Zhang, J., Lu, X., Wan, N., Hua, Z., Wang, Z., Huang, H., Yang, M., Wang, F., 2014 Mar. 68Ga-DOTA-NGR as a novel molecular probe for APN-positive tumor imaging using MicroPET. Nucl. Med. Biol. 41 (3), 268–275. https://doi.org/10.1016/j.nucmedbio.2013.12.008. Epub 2013 Dec 18. PMID: 24438818.

Zhao, M., Yang, W., Zhang, M., Li, G., Wang, S., Wang, Z., Ma, X., Kang, F., Wang, J., 2016 Sep. Evaluation of ^{68}Ga-labeled iNGR peptide with tumor-penetrating motif for microPET imaging of CD13-positive tumor xenografts. Tumour Biol. 37 (9), 12123–12131. https://doi.org/10.1007/s13277-016-5068-0. Epub 2016 May 24. PMID: 27220318.